JOURNAL OF CATALYSIS 107, 307–316 (1987)

Propylene Oxidation to Acrolein on Fe–Sb–Ti–O Catalysts

M. CARBUCICCHIO,* G. CENTI,† P. FORZATTI,‡ F. TRIFIRÒ,† AND P. L. VILLA‡

*Dipartimento di Fisica, Università di Parma, Parma, Italy; †Dipartimento di Chimica Industriale e dei Materiali, Università di Bologna, Bologna, Italy; and ‡Dipartimento di Chimica Industriale ed Ingegneria Chimica, Politecnico di Milano, Milano, Italy

Received July 9, 1986; revised March 25, 1987

Coprecipitated Fe–Sb–Ti mixed oxides with an (Fe + Sb)/(Fe + Sb + Ti) atomic ratio in the 0–1 range and with an Sb/Fe atomic ratio of 2.0 were characterized by means of X-ray diffraction, Mössbauer, and infrared spectroscopies and by attrition resistance tests. Catalysts were tested in the oxidation of propene to acrolein. Catalysts with high and similar selectivities (80–90%) are obtained in the 0.3–1.0 (Fe + Sb)/(Fe + Sb + Ti) atomic ratio range where X-ray diffraction analysis shows the presence of either only a single crystalline rutile phase or a single rutile phase together with α- and β-Sb_2O_4 in variable amounts. No correlation was found between selectivity to acrolein and the presence of crystalline Sb_2O_4. On the contrary, selectivity to acrolein seems to be associated with Sb ions stabilized at the surface of the catalyst. The results of physicochemical characterization and interpretation thereof are consistent with the crystalline rutile-like single phase being constituted by a solid solution originating from either $FeSbO_4$, $FeSbO_4$ doped with Ti, and TiO_2 doped with Fe and Sb phases, or a lattice of largely uniform periodicity, but with localized variations in composition.

INTRODUCTION

Iron–antimony mixed oxides supported on silica and promoted with small quantities of Te, Mo, and other elements represent an important class of commercial catalysts for the ammoxidation of propene to acrylonitrile (*1*, *2*). The use of silica as support ensures good attrition characteristics and results in an appropriate catalyst density which allows the commercial process to be operated in fluidized bed reactors. The stability with use of these catalysts, however, is not completely satisfactory due to the formation of fine particles associated with the loss of antimony oxides from the catalyst.

One might expect that more stable catalysts could be prepared if a stronger interaction of the iron–antimony oxides with the support is realized. In this respect it is worth noting that (i) the only crystalline phases detected in iron–antimony mixed oxides are $FeSbO_4$ and Sb_2O_4 (*3*), (ii) $FeSbO_4$ is isotypic with the rutile modification of TiO_2, (iii) Sb_2O_4 forms a solid solution with rutile TiO_2 (up to about 5 wt% of Sb_2O_4) at 1073–1173 K (*4*).

This situation led us to investigate the ternary titanium–iron–antimony oxide system (*5*). The catalysts were prepared by coprecipitation in order to obtain an intimate mixture of the three components. The (Fe + Sb)/(Fe + Sb + Ti) atomic ratio quoted in the following as AP/APS [(active phase)/(active phase + support)] was varied in the 0–1 range, whereas the Sb/Fe atomic ratio was usually kept constant and equal to 2, the optimal value of unsupported iron–antimony mixed oxides (*6*). The Sb-based catalysts normally utilized in allylic oxidation and ammoxidation reactions, such as Fe–Sb–O and Sn–Sb–O, are typically constituted by a phase with rutile structure and by crystalline Sb_2O_4 (*6*, *7*). Starting from this observation some authors concluded that both phases are required to ensure good catalytic performance and suggested that the active species are associated with grain boundaries (*8*), an

0021-9517/87 $3.00

oriented α-Sb_2O_4 layer (*9, 10*), or phase cooperation (*11*). Other authors, however, identified the active sites with couples of Sb ions stabilized in specific arrangements at the surface of the rutile phase and considered α-Sb_2O_4 a collateral inactive phase (*3, 6, 12*). By diluting the active phase (iron–antimonate) with an isostructural oxide (TiO_2) it is thus possible to compare better these two literature hypotheses on the nature of the selective sites present in the iron–antimonate and, more generally, on Sb-based catalysts with rutile structure.

EXPERIMENTAL

Preparation of Catalysts

The catalysts were prepared by dropping an aqueous $FeCl_3 \cdot 6H_2O$ solution into a $TiCl_4$–$SbCl_5$ mixture kept at 363 K under nitrogen and contained in a glass vessel provided with a stirrer and four internal baffles on the wall to ensure perfect mixing of the liquid. Different relative quantities of Fe, Sb, and Ti salts were used depending on the desired Sb/Fe and (Fe + Sb)/(Fe + Sb + Ti) atomic ratios. The resulting solution was neutralized with NH_4OH, 30% by volume, to give an equilibrium pH value of 8. The slurry was aged for 2 h under stirring at 363 K, filtered, washed twice with boiling water, dried at 403 K for 48 h, and calcined at 623 K (ramp 100 K/h; hold 16 h) and finally at 1173 K (ramp 50 K/h; hold 3 h). A few alternative preparations were performed with final calcination temperatures of 1073 K (ramp 50 K/h; hold 3 h) and 973 K (ramp 50 K/h; hold 1.5 h).

A reference sample with AP/APS = 0.3 and Sb/Fe = 2.0 was also prepared by impregnating a rutile TiO_2 support (Trioxide CLDD 1587/4; S = 29 $m^2\ g^{-1}$) with concentrated Fe(III)–nitrate solution, followed by drying at 423 K, calcination at 673 K, again impregnation with liquid $SbCl_5$ under anhydrous atmosphere, hydrolysis by addition onto the solid of a few drops of double-distilled water, drying, and calcination as above.

Characterization of Catalysts

X-ray powder diffraction patterns were recorded with a Philips computer-controlled diffractometer using Ni-filtered Cu$K\alpha$ radiation. Data were collected at 0.01° 2ϑ increments. Cell parameters were estimated by a least-squares method using the eight most intense reflections of the rutile phase.

Mössbauer absorption spectra of the ^{57}Fe 14.4-keV radiation were measured by means of a constant acceleration spectrometer and a source of 25-mCi ^{57}Co in a Rh matrix. The spectra were fitted by superimposing a series of Lorentzian lines.

Infrared spectra (KBr disk technique) were recorded on a JASCO A202 spectrophotometer. The TiO_2 contribution to each spectrum was subtracted by using in the KBr reference disk the same weight amount of TiO_2 as was present in the examined Fe–Sb–Ti sample. The relative weight amount of the active phase with respect to KBr was kept constant and equal to 1.1%, w/w.

The attrition resistance characteristics of the samples were investigated by means of the test described by Forsythe and Hertwig (*13*). In this laboratory-accelerated attrition test, a catalyst sample is subjected to a jet attrition action for 1 h. The resulting changes in the distribution of catalyst particle size, determined by a screen analysis, are taken as a measure of the attrition characteristics and compared with that of a commercial fluidized bed catalyst. Microspheroidal silica was assumed as a commercial catalyst due to its large use in fluidized bed applications. The attrition apparatus and the test procedure have already been reported elsewhere (*14*).

Catalytic Activity

The oxidation of propylene was accomplished in an AISI 316 SS fixed bed reactor (i.d. 5.4 mm) provided with an axial thermocouple sliding inside a tube of 1.2 mm o.d. The catalyst charge ranged between 5

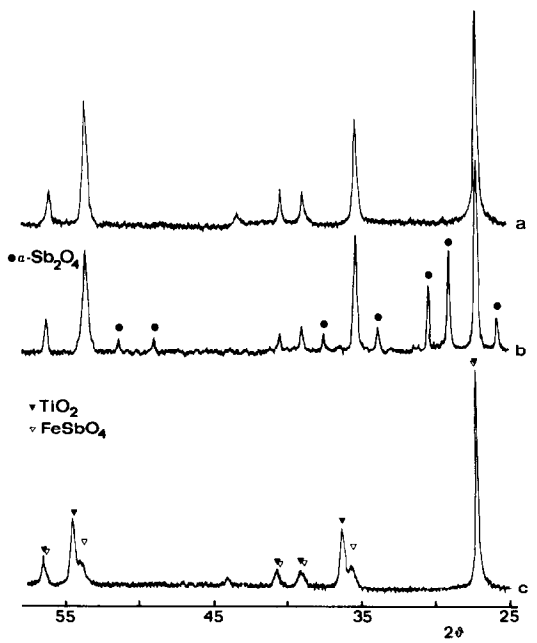

FIG. 1. X-ray diffraction patterns of Fe–Sb–Ti catalysts: (a) coprecipitated, AP/APS = 0.3, calcination temperature 1173 K; (b) coprecipitated, AP/APS = 0.75, calcination temperature 1173 K; (c) impregnated, AP/APS = 0.30, calcination temperature 1103 K.

and 7 g and the catalyst particle size was 35–52 mesh. The feed consisted of 6% C_3H_6, 13% O_2 (the balance being N_2) usually at 140–200 ml min^{-1} (at STP) total gas flow. The pressure at the reactor inlet was typically 1.35–1.45 atm. Details for the analysis of reagents and products have been reported elsewhere (*15*).

RESULTS

X-Ray Diffraction (XRD)

The catalysts prepared by coprecipitation and calcined at 1173 K show the diffraction lines typical of a rutile phase (Fig. 1a). Two distinct rutile phases (TiO_2 and $FeSbO_4$) are present in a catalyst prepared by impregnation on a preformed TiO_2 (Fig. 1c). The unit cell parameters and the cell volume of the rutile phase in coprecipitated catalysts show an almost linear increase with AP/APS, with a deviation from linearity in the 0.5–0.8 AP/APS range (Fig. 2). Above AP/APS equal to 0.5 the XRD lines of pure antimony oxides are also detected, in addition to those of the rutile phase (Fig. 1b). The relative intensities of the main characteristic lines of α- and β-Sb_2O_4 are reported in Fig. 3 as a function of the active phase content. Both α- and β-Sb_2O_4 were detected in pure iron–antimony mixed oxide, whereas only α-Sb_2O_4 was monitored for AP/APS beyond 0.9, with a maximum at AP/APS = 0.75. The XRD lines of antimony oxides were never observed in samples calcined at temperatures equal to or lower than 1073 K.

The XRD lines of an anatase phase were

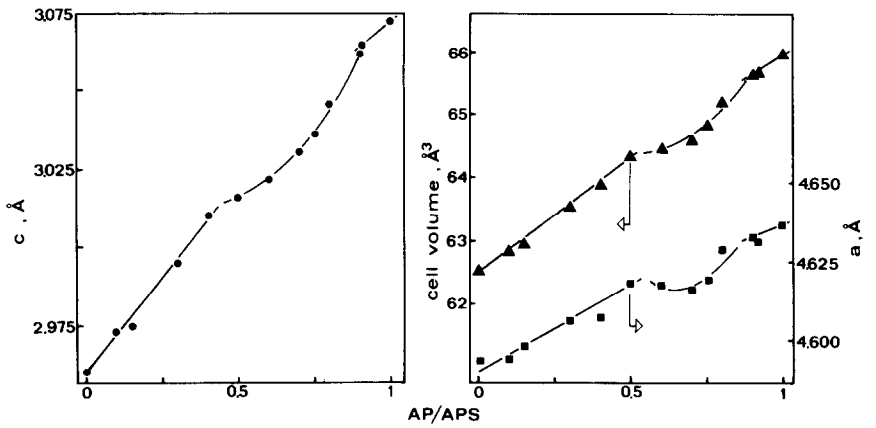

FIG. 2. Cell parameters and volume of rutile phase as a function of AP/APS ratio; catalysts calcined at 1173 K.

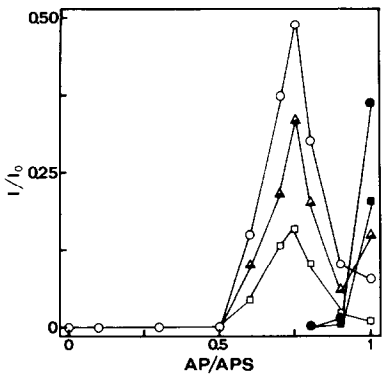

FIG. 3. Relative intensities (with respect to the (110) reflection of the rutile phase) of the main peaks of α-Sb_2O_4 and of β-Sb_2O_4 as a function of AP/APS; catalysts calcined at 1173 K. α-Sb_2O_4: (○) (112) reflection, (□) (111) reflection. β-Sb_2O_4: (●) (111) reflection, (■) (311) reflection. α- and β-Sb_2O_4: (▲) (004) reflection of α-Sb_2O_4 and (400) reflection of β-Sb_2O_4.

observed in catalysts with an AP/APS ratio lower than 0.3 and calcined at low temperatures. On increasing the calcination temperature, the system evolves toward a single rutile phase, as shown in Fig. 4A. The anatase to rutile transition temperature increases by lowering the active phase content. This is shown in Fig. 4B for catalysts with AP/APS up to 0.3. Catalysts with AP/APS higher than 0.3 and calcined at 773 K present only the rutile phase; at lower calcination temperatures a pseudo-amorphous pattern is observed.

Mössbauer Spectroscopy

Figures 5a, 5b, and 5c show the Mössbauer spectra measured for coprecipitated catalysts calcined at 1173 K with AP/APS = 1.0, 0.5, and 0.15, respectively. Spectrum (a) is typical of $FeSbO_4$ mixed oxide and, according to Refs. (*3, 12*), it can be interpreted as the superposition of two quadrupole doublets: a low-intensity one due to octahedral high-spin Fe^{2+} ions and a predominant one due to distorted octahedral high-spin Fe^{3+} ions. By lowering the AP/APS ratio (spectra (b and c)), the Mössbauer spectra change considerably. A possible interpretation is that contributions from Fe^{3+} ions located in a distribution of nonequivalent lattice sites are superimposed on the spectrum of $FeSbO_4$. To fit the spectra, only two kinds of nonequivalent iron sublattices were assumed, the corresponding two quadrupole doublets (β contribution in spectra (b and c)) having linewidths greater than those of natural ^{57}Fe nuclei. From this analysis it follows that, by decreasing the AP/APS ratio, the contribution from pure $FeSbO_4$ (α) decreases whereas the relative amount of the iron species responsible for the inner doublet of the β contribution increases. Accordingly the Mössbauer data suggest that different situations occur depending on the AP/APS value. For AP/APS $\cong$ 1.0, the iron sublattices of the catalyst are those of pure Fe SbO_4 (α contribution to the spectra) with Ti dopant as nearest neighbors (larger doublet of β contribution). For AP/APS close to zero the catalyst is mainly constituted by TiO_2 doped with Fe and Sb (inner doublet

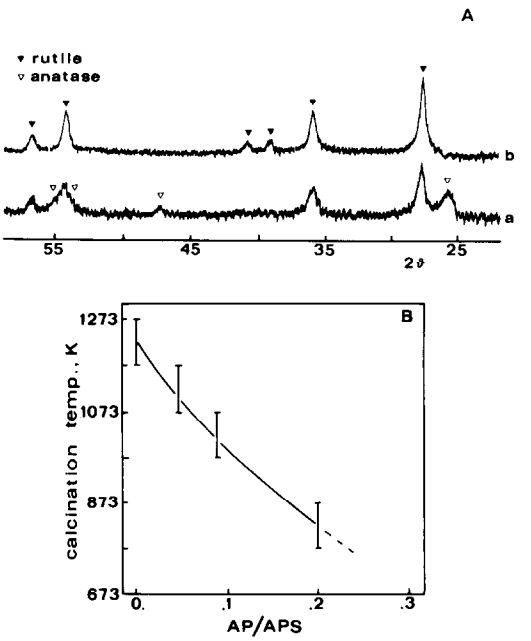

FIG. 4. (A) X-ray diffraction patterns of coprecipitated catalysts with AP/APS = 0.2; final calcination temperature (a) 823 K for 3 h, (b) 873 K for 3 h. (B) Temperature range of anatase to rutile transition in coprecipitated catalysts as a function of AP/APS.

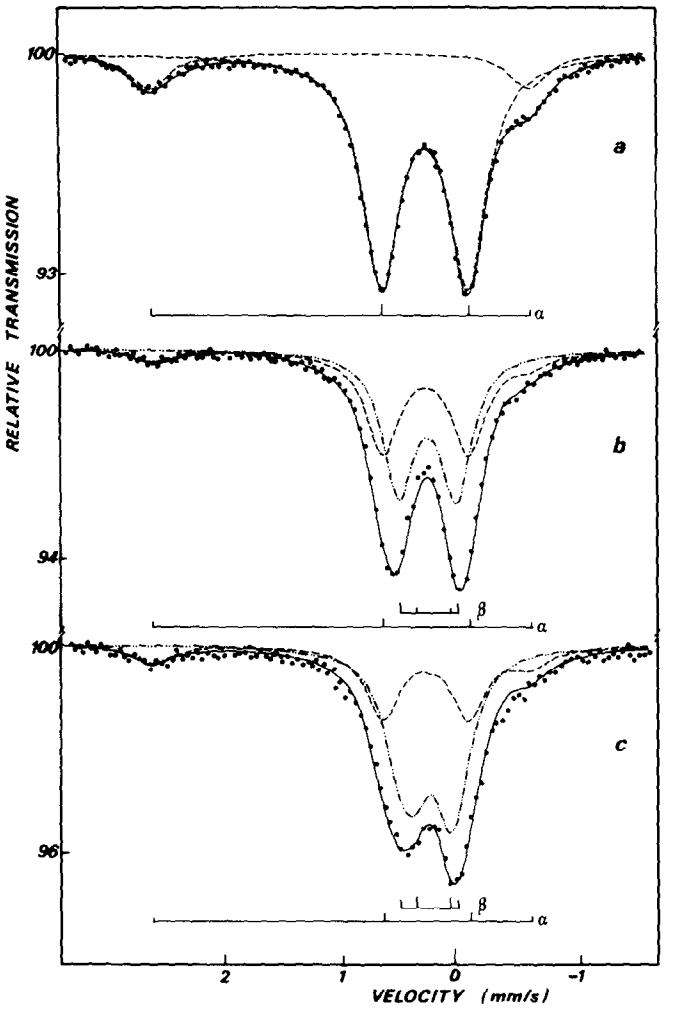

FIG. 5. Mössbauer spectra of coprecipitated catalysts calcined at 1173 K. (a) AP/APS = 1.0; (b) AP/APS = 0.5; (c) AP/APS = 0.15.

of the β contribution). For intermediate AP/APS values the iron sublattices of Fe SbO_4 pure and Ti doped coexist with those of Fe (and Sb) doped TiO_2, the mutual relative amounts depending on AP/APS.

It should be noted that the Mössbauer spectrum measured for AP/APS = 0.3 impregnated catalyst shows contributions similar to those for coprecipitated catalysts with AP/APS lower than 1.0 and is consistent with the above interpretation. In this case, however, the situation is significantly different: a layer of iron–antimony mixed oxides can form on TiO_2 so that a TiO_2 phase containing Fe and Sb prevails at the interface on the support side whereas a $FeSbO_4$ phase containing Ti prevails on the iron–antimony mixed oxide side.

Infrared Spectra

Figure 6 gives the infrared spectra, after subtraction of the TiO_2 contribution, of coprecipitated Fe–Sb–Ti samples calcined at 1173 K. The spectrum of pure active phase exhibits principal bands in the 500- to 750-cm^{-1} region connected with the stretching mode of νSbO in SbO_6 octahedra, of $FeSbO_4$ (bands at 660 and 520 cm^{-1} (*3*, *16–19*)), and of distorted octahedra and tetrahedra of Sb(V) and Sb(III) in α- and

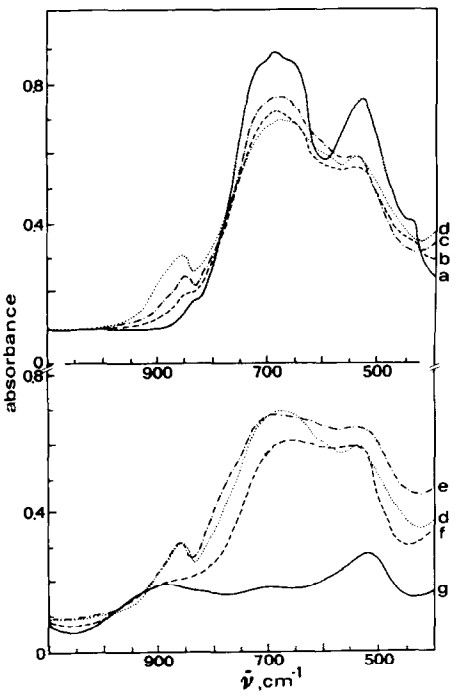

FIG. 6. Infrared spectra (after TiO_2 subtraction) of coprecipitated catalysts calcined at 1173 K. (a) AP/APS = 1.0; (b) AP/APS = 0.75; (c) AP/APS = 0.60; (d) AP/APS = 0.50; (e) AP/APS = 0.30; (f) AP/APS = 0.15; (g) AP/APS = 0.09.

β-Sb_2O_4 (bands at 750, 650, 610, and 440–420 cm^{-1} (*9*, *20*)). The weak absorption at about 830 cm^{-1} has been attributed to Sb(V)=O double bond stretching (*20*) or to a combination band (*19*). This absorption is also present in Sb_6O_{13} as well as in a wide class of antimonates which are known to be active catalysts for selective allylic oxidation and ammoxidation reactions (*6*), but not in α- and β-Sb_2O_4. By decreasing the amount of the active phase from AP/APS = 1.0 down to 0.5 the following IR features become manifest. (i) The relative intensity of the bands in the 500- to 750-cm^{-1} region changes and the absorption centered at 440 cm^{-1} disappears. Both these effects can be attributed to the different amounts of α- and β-Sb_2O_4 present in the samples and are in line with the XRD results. (ii) The absorption originally centered at 830 cm^{-1} increases in intensity and progressively shifts to slightly higher frequencies. This suggests that a modification of the Sb–O geometry occurs by decreasing the active phase content down to AP/APS = 0.5.

For AP/APS lower than 0.5 the IR spectra show the following main features. (i) Starting from AP/APS = 0.15 the absorption originally centered at 860 cm^{-1} decreases in intensity, shifts to higher frequencies, and is less resolved. (ii) The relative intensity of the absorption maxima in the 500- to 750-cm^{-1} region varies and the absorption at 520 cm^{-1} becomes the most intense for AP/APS = 0.09.

Figure 7 reports the infrared spectra of coprecipitated and impregnated catalysts calcined at 1173 K with AP/APS = 0.3. Inspection indicates that the absorption at 860 cm^{-1} is more intense in the coprecipitated catalyst, which eventually confirms that the coprecipitation method results in a higher degree of interaction between the catalyst constituents.

Catalytic Tests

Figure 8 shows the results of propylene oxidation over coprecipitated catalysts as a function of the AP/APS ratio. The activity increases almost linearly with the (Fe + Sb) content; however, a deviation from linearity is evident in the 0.5–0.8 AP/APS range. The selectivity to acrolein increases and

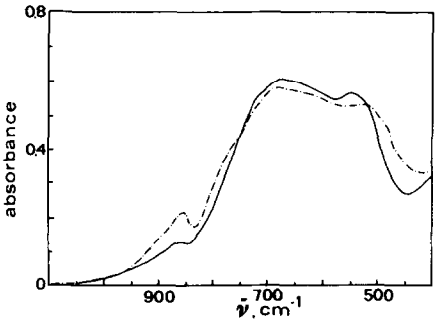

FIG. 7. Comparison of infrared spectra (after TiO_2 subtraction) of coprecipitated (dotted line) and impregnated (full line) catalysts with AP/APS = 0.30 (calcination temperature 1173 K).

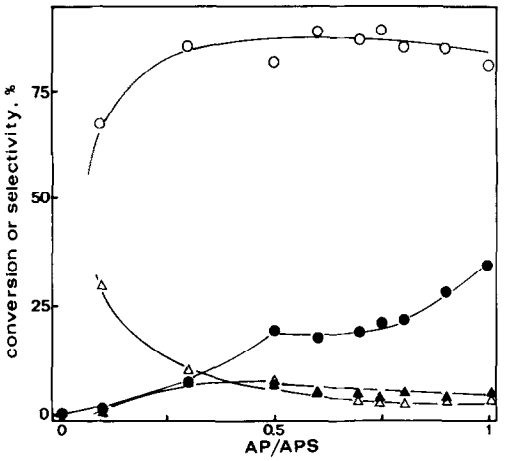

FIG. 8. Oxidation of propylene as a function of AP/APS over coprecipitated catalysts calcined at 1173 K. Experimental conditions: T = 663 K, P = 1.3–1.4 atm, F = 140–200 ml min^{-1}, $W_{cat.}$ = 5–7 g. Legend: (●) propylene conversion, (○) selectivity to acrolein, (▲) selectivity to CO_2, (△) selectivity to CO.

reaches a high and almost constant value (about 80–90%) already at AP/APS = 0.3.

The effect of calcination temperature and of the Sb/Fe atomic ratio upon the catalytic behavior of Fe–Sb–Ti coprecipitated catalysts is shown in Figs. 9 and 10. A drastic increase in the selectivity to acrolein is

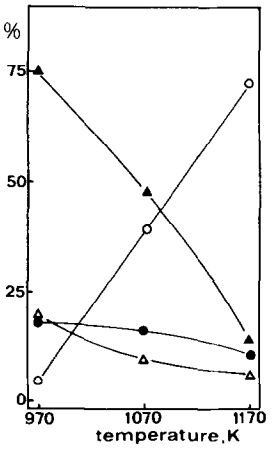

FIG. 9. Effect of calcination temperature of coprecipitated catalysts with AP/APS = 0.3 and Sb/Fe = 2.0 on the catalytic behavior in propylene oxidation. Experimental conditions: T = 693 K, P = 1.4–1.5 atm, $W_{cat.}$ = 6 g, F = 200–260 ml min^{-1}. Legend as in Fig. 8.

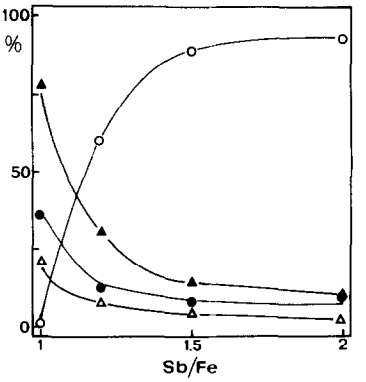

FIG. 10. Effect of Sb/Fe atomic ratio at constant Fe/Ti atomic ratio (1/3) and calcination temperature (1173 K) on catalytic behavior in propylene oxidation for coprecipitated catalysts. Experimental conditions: T = 633 K, P = 1.4–1.5 atm, $W_{cat.}$ = 6 g, F = 200–250 ml min^{-1}. Legend as in Fig. 8.

observed by increasing the calcination temperature, and especially at the expense of carbon dioxide. On the other hand, the propylene conversion decreases only slightly, which is not in line with the marked decrease in surface area. By increasing the Sb/Fe atomic ratio and by keeping the AP/APS ratio constant and equal to 0.5, a decrease in both propylene conversion and selectivity to carbon oxides is observed together with a corresponding increase in selectivity to acrolein. Constant catalytic performances are reached already at Sb/Fe = 1.5.

Attrition Tests

The results of the attrition tests are reported in Table 1 for two coprecipitated catalysts calcined at 1173 K with AP/APS = 0.3 and 0.5, respectively, and for Grace 951 microspheroidal silica. The similar productions of fine particles (lower than 0.044 mm) measured after Forsythe tests indicate that the attrition characteristics of the Fe–Sb–Ti oxide system are comparable with those of a commercial fluidized bed material and that they are little influenced by the amount of active phase, at least up to AP/APS = 0.5.

TABLE 1

Attrition Tests (Forsythe Method (*13*)) for Coprecipitated Catalysts

Screen analysis[a]	Reference (Grace 951 silica)		Coprecipitated samples			
			AP/APS = 0.30		AP/APS = 0.50	
	(a)[b]	(b)[c]	(a)	(b)	(a)	(b)
+0.0125 mm	0.12	0.08	0.12	0.12	0.12	0.12
−0.125 +0.074 mm	3.20	2.42	3.20	2.78	3.20	2.67
−0.074 +0.063 mm	24.78	14.25	24.78	19.49	24.78	19.30
−0.063 +0.053 mm	2.51	3.20	2.51	3.48	2.51	3.45
−0.053 +0.044 mm	48.03	24.98	48.03	21.80	48.03	23.83
−0.044 mm	21.35	55.05	21.35	50.88	21.35	51.88

[a] (+) higher than; (−) less than.
[b] Before attrition tests.
[c] After attrition tests.

DISCUSSION

Characteristics of the Fe–Sb–Ti–O System

The results of XRD analysis and of catalytic measurements indicate that it is possible to prepare crystalline single-phase selective catalysts if (i) the coprecipitation method described is adopted (compare Figs. 1a and 1c), (ii) the active phase content is maintained within the 0.3–0.5 AP/APS range (Figs. 2, 3, and 8), (iii) the calcination temperature is about 1173 K (Fig. 9), and (iv) the Sb/Fe atomic ratio is higher than 1.5 (Fig. 10). Catalysts with these properties present good attrition characteristics (Table 1) and are suitable for use in fluidized bed reactors.

The presence of only the lines typical of a rutile phase and the almost linear increase in the cell parameters with the AP/APS ratio clearly indicate the formation of a crystalline solid solution of Fe and Sb oxides in rutile TiO_2. However, the marked changes of the highest frequency IR absorption and of the relative intensities of the absorption maxima (500- to 750-cm^{-1} region) in the range $0 < AP/APS \lesssim 0.3$ and the regular changes of the above IR features for higher AP/APS values indicate that the geometry of Sb–O bonds modifies on increasing the active phase content in a more complex way than that suggested from XRD. Moreover, the Mössbauer analyses suggest a complex situation of Fe^{3+} nonequivalent sites which modifies with AP/APS, and specifically suggest the presence of Fe^{3+} sublattices equivalent to those in pure $FeSbO_4$ also in the samples with AP/APS = 0.5 and 0.15. The above data and their interpretations are consistent with the view that the solid solution evidenced by the XRD analysis originates either from a mutual intergrowth (*21*) of $FeSbO_4$, $FeSbO_4$–Ti doped, and TiO_2–Fe (and Sb) doped rutile-like phases or from a lattice of largely uniform periodicity but with localized variations in composition as far as Fe sublattices are considered.

By increasing the active phase content above AP/APS = 0.5 the following marked changes in the physicochemical properties were monitored: (i) antimony oxide is segregated first as α-Sb_2O_4; (ii) parallel with this effect, the cell volume of the rutile phase and the propylene conversions are significantly smaller than expected based on the trends present at lower active phase contents; (iii) the IR and Mössbauer features change from the characteristic ones of

Fe–Sb–Ti solid solution to those of iron–antimony mixed oxides; and (iv) for AP/APS above 0.8 antimony oxide is segregated mainly in the form of β-Sb_2O_4. All these data can be explained assuming that for low AP/APS values the primary rutile structure is that of TiO_2 which is expanded by the incorporation of Fe and Sb ions to form the Fe–Sb–Ti solid solution. The incorporation of Sb^{3+} appears to be most critical based on its ionic radius and because of this, segregation of α-Sb_2O_4 is observed for AP/APS > 0.5. This finally results in a marked discontinuity of the cell volume of the rutile phase as well as of surface area and propylene conversion. The segregation of antimony oxide in the form of β-Sb_2O_4 for AP/APS > 0.8 suggests that the catalysts with high active phase contents should more likely be regarded as constituted primarily by a $FeSbO_4$ rutile structure modified by the incorporation of Ti ions.

Nature of Active Species

Two hypotheses can be found in the literature about the nature of the selective species on Sb-based catalysts: (i) the selective sites form at the interface of two crystalline phases (Sb doped rutile phase and Sb_2O_4) (*8–11*), and (ii) the selective site is Sb stabilized in a specific arrangement at the surface of the rutile phase (*3, 6, 12*).

In the case of the Fe–Sb–Ti oxide system it was possible to prepare catalysts with similar and high selectivities to acrolein. In these catalysts crystalline Sb_2O_4 ($0.3 \leq$ AP/APS ≤ 0.5) is not present, α-Sb_2O_4 ($0.6 \leq$ AP/APS ≤ 0.8) is present alone, or both α-Sb_2O_4 and β-Sb_2O_4 ($0.9 \leq$ AP/APS ≤ 1.0) are present. Furthermore, the catalysts do not show any specific orientation of α-Sb_2O_4 crystallites (Fig. 3). Therefore no correlation was found in our catalysts between selectivity to acrolein and the presence of crystalline Sb_2O_4, a specific orientation of α-Sb_2O_4, or phase cooperation on the other side. Our data are more consistent with the active species for allylic oxidation being associated with antimony ions stabilized on the surface of the rutile phase (*6*). This picture is also in line with the effect of calcination temperature and Sb/Fe ratio upon selectivity to acrolein inasmuch as these effects can probably be explained by assuming a surface enrichment of antimony (*22, 23*).

ACKNOWLEDGMENT

This work was supported by a financial grant from DSM (Geleen, The Netherlands) which is gratefully acknowledged.

REFERENCES

1. Yoshino, T., Saito, S., Sasaki, Y., and Nakamura, Y., U.S. Patent 3,657,155 (1972); 3,686,138 (1972).
2. Callahan, J. L., Heights, B., Grasselli, R. K., and Knipple, W. R., U.S. Patent 3,546,138 (1970).
3. Carbucicchio, M., Centi, G., and Trifirò, F., *J. Catal.* **91,** 85 (1985).
4. Zenkovets, G. A., Tarasova, D. V., Andrushkevich, T. V., Aleshina, G. I., Nikoro, T. A., and Ravilov, R. G., *Kinet. Catal.* **20,** 380 (1979).
5. Forzatti, P., Villa, P., and Trifirò, F., Eur. Pat. Appl. 832001986 (1983).
6. Centi, G., and Trifirò, F., *Catal. Rev. Sci. Eng.* **28,** 165 (1986).
7. Berry, F., *Adv. Catal.* **30,** 97 (1981).
8. Fattore, V., Fuhrman, Z. A., Manara, G., and Notari, B., *J. Catal.* **37,** 223 (1975).
9. Volta, J. C., Bussière, P., Coudurier, G., Herrmann, J. M., and Védrine, J. C., *Appl. Catal.* **16,** 315 (1985).
10. Portefaix, J. L., Bussière, P., Forissier, M., Figueras, F., Friedt, J. M., Sanchez, J. P., and Theobald, F., *J. Chem. Soc. Faraday Trans. 1* **76,** 1652 (1980).
11. Teller, R. G., Brazdil, J. F., and Grasselli, R. K., *J. Chem. Soc. Faraday Trans. 1* **81,** 1693 (1985).
12. Burriesci, N., Garbassi, F., Petrera, M., and Petrini, G., *J. Chem. Soc. Faraday Trans. 1* **78,** 817 (1982).
13. Forsythe, W., and Hertwig, W. R., *Ind. Eng. Chem.* **41,** 1200 (1949).
14. Cairati, L., Di Fiore, L., Forzatti, P., Pasquon, I., and Trifirò, F., *Ind. Eng. Chem. Process Des. Dev.* **19,** 561 (1980).
15. Forzatti, P., Villa, P. L., Ferlazzo, N., and Jones, D., *J. Catal.* **76,** 188 (1982).
16. Rocchiccioli-Deltcheff, C., Dupuis, T., Frank, R., Harmelin, M., and Wadier, C., *C.R. Acad. Sci. Paris B,* 541 (1970).

17. Husson, E., Repelin, Y., and Brusset, H., *Spectrochim. Acta A* **35,** 1177 (1979).
18. Husson, E., Repelin, Y., and Vanderborre, M. T., *Spectrochim. Acta A* **40,** 1017 (1984).
19. Frank, R., Rocchiccioli-Deltcheff, C., and Guillermet, J., *Spectrochim. Acta A* **30,** 1 (1974).
20. Sala, F., and Trifirò, F., *J. Catal.* **34,** 68 (1974).
21. Rao, C. N. R., and Thomas, J. M., *Acc. Chem. Res.* **18,** 113 (1985).
22. Boudeville, Y., Figueras, F., Forissier, M., Portefaix, J. L., and Védrine, J. C., *J. Catal.* **58,** 52 (1979).
23. Egdell, R. G., Flavell, W. R., and Taverner, P., *J. Solid State Chem.*, 51 (1984).